

Observation of a 4-spin Plaquette Singlet State in the Shastry–Sutherland compound $\text{SrCu}_2(\text{BO}_3)_2$

M.E. Zayed^{1,2,3}, Ch. Rüegg^{3,4}, J. Larrea J.^{2,5}, A.M. Läuchli⁶, C. Panagopoulos^{7,8}, S.S. Saxena⁷, M. Ellerby⁹, D.F. McMorrow⁹, Th. Strässle³, S. Klotz¹⁰, G. Hamel¹⁰, R.A. Sadykov^{11,12}, V. Pomjakushin³, M. Boehm¹³, M. Jiménez–Ruiz¹³, A. Schneidewind¹⁴, E. Pomjakushina¹⁵, M. Stingaciu¹⁵, K. Conder¹⁵, and H.M. Rønnow²

¹ Department of Mathematics, Statistics and Physics,

College of Arts and Science, Qatar University, P.O. Box 2713 Doha, Qatar

² Laboratory for Quantum Magnetism, Ecole Polytechnique Fédérale de Lausanne (EPFL), 1015 Lausanne, Switzerland

³ Laboratory for Neutron Scattering and Imaging,

Paul Scherrer Institut, 5232 Villigen PSI, Switzerland

⁴ Department of Quantum Matter Physics, University of Geneva, 1211 Geneva 4, Switzerland

⁵ Centro Brasileiro de Pesquisas Físicas, Rua Doutor Xavier Sigaud 150, CEP 2290-180, Rio de Janeiro, Brazil

⁶ Institut für Theoretische Physik, Universität Innsbruck, 6020 Innsbruck, Austria

⁷ Cavendish Laboratory, University of Cambridge, Cambridge CB3 0HE, UK

⁸ Division of Physics and Applied Physics, School of Physical and Mathematical Sciences,

Nanyang Technological University, Singapore 637371

⁹ London Centre for Nanotechnology and Department of Physics and Astronomy,

University College London, London WC1E 6BT, UK

¹⁰ IMPMC; CNRS–UMR 7590, Université Pierre et Marie Curie, 75252 Paris, France

¹¹ Institute for Nuclear Research, Russian Academy of Sciences,

prospekt 60-letiya Oktyabrya 7a, Moscow 117312.

¹² Vereshchagin Institute for High Pressure Physics,

Russian Academy of Sciences, 142190 Troitsk, Russia

¹³ Institut Laue-Langevin, 71 avenue des Martyrs - CS 20156- 38042 Grenoble Cedex 9, France

¹⁴ Jülich Centre for Neutron Science (JCNS), Forschungszentrum Jülich GmbH,

Outstation at Heinz Maier-Leibnitz Zentrum (MLZ),

Lichtenbergstraße 1, D-85747 Garching, Germany

¹⁵ Laboratory for Scientific Developments and Novel Materials,

Paul Scherrer Institut, 5232 Villigen PSI, Switzerland

(Dated: August 29, 2018)

The study of interacting spin systems is of fundamental importance for modern condensed matter physics. On frustrated lattices, magnetic exchange interactions cannot be simultaneously satisfied, and often give rise to competing exotic ground states¹. The frustrated 2D Shastry–Sutherland lattice² realized by $\text{SrCu}_2(\text{BO}_3)_2$ ³ is an important test to our understanding of quantum magnetism. It was constructed to have an exactly solvable 2-spin dimer singlet ground state within a certain range of exchange parameters and frustration. While the exact dimer state and the antiferromagnetic order at both ends of the phase diagram are well known, the ground state and spin correlations in the intermediate frustration range have been widely debated^{2–12}. We report here the first experimental identification of the conjectured plaquette singlet intermediate phase in $\text{SrCu}_2(\text{BO}_3)_2$. It is observed by inelastic neutron scattering after pressure tuning at 21.5 kbar. This gapped plaquette singlet state with strong 4-spin correlations leads to a transition to an ordered Néel state above 40 kbar, which can realize a deconfined quantum critical point.

In the field of quantum magnetism, geometrically frus-

trated lattices generally imply major difficulties in analytical and numerical studies. For very few particular topologies however, it has been shown that the ground state, at least, can be calculated *exactly* as for the Majumdar–Gosh model¹³ that solves the J_1 – J_2 zig-zag chain when $J_1 = 2J_2$. In 2D, the Shastry–Sutherland model² consisting of an orthogonal dimer network of spin $S=1/2$ was developed in order to be exactly solvable. For an inter-dimer J' to intra-dimer J exchange ratio $\alpha \equiv J'/J \leq 0.5$ the ground state is a product of singlets on the strong bond J . Numerical calculations have further shown that this remains valid up to $\alpha \leq \sim 0.7$ and for small values of 3D couplings J'' between dimer layers. At the other end, for $\sim 0.9 \leq \alpha \leq \infty$ the system approaches the well known 2D square lattice, which is antiferromagnetically (AFM) ordered, albeit with significant quantum fluctuations that are believed to include resonating singlet correlations resulting in fractional excitations¹⁴. The phase diagram of the Shastry–Sutherland model, both with and without applied magnetic field, has been intensively studied by numerous theoretical and numerical approaches³. In the presence of magnetic field, magnetization plateaus at fractional values of the saturation magnetization corresponding to Mott insulator phases of dimer states, as well as possible superfluid and super-solid phases have been extensively studied^{6,15,16}. At zero field, the main unsolved issue is the existence and nature

of an intermediate phase for $\sim 0.7 \leq \alpha \leq \sim 0.9$. A variety of quantum phases and transitions between them have been predicted depending on the theoretical technique used: a direct transition from dimer singlet phase to AFM order^{2,5,6}, or an intermediate phase with helical order⁴, columnar dimers¹⁰, valence bond crystal¹¹ or resonating valence bond (RVB) plaquettes^{8,9}. Recent results indicate that a plaquette singlet phase is favored^{3,17}. From such a phase, which would have an additional Ising-type order parameter, a subsequent transition to AFM order could provide a realisation of the so far elusive deconfined quantum critical point¹⁸.

The compound strontium copper borate $\text{SrCu}_2(\text{BO}_3)_2$ is the only known realization of the Shastry-Sutherland model with $S=1/2$ spins³ and has thus triggered considerable attention in the field of quantum magnetism. The spectrum of $\text{SrCu}_2(\text{BO}_3)_2$ exhibits an almost dispersionless $\Delta=3$ meV gap, and a bound-state of two triplets (BT) forms at $E_{BT} \simeq 5$ meV. The unusual size and dispersionless nature of the gap is an effect of the frustration which prevents triplets from hopping up to sixth order³. The estimated exchange parameters in the material $J \sim 85$ K and $\alpha = 0.635^3$ or $J \sim 71$ K and $\alpha = 0.603^7$ place the compound close to an interesting regime $\alpha \sim 0.7$ where correlations may change dramatically at a critical point.

A precious mean to tune a quantum magnet across a quantum phase transition is the application of hydrostatic pressure as it directly modifies the atomic distances and bridging angles, such as Cu-O-Cu and thus the magnetic exchange integrals. Quantum phase transitions were successfully discovered in dimer magnets upon application of pressure¹⁹. However high pressure measurements remain technically challenging. In the case of $\text{SrCu}_2(\text{BO}_3)_2$ magnetic susceptibility²⁰ and ESR²¹ to moderate pressures ($p \leq 12$ kbar) indicate a softening of the gap, while the combined effect of pressure and field was measured by susceptibility and NMR²². In the latter case magnetic order occurring at 24 kbar and 7 T on a fraction of the dimers was proposed. In an X-ray diffraction investigation the temperature dependence of the lattice parameters was analysed as an indirect proxy for the singlet triplet gap leading to the suggestion that it closes at 20 kbar²³. At even higher pressures neutron and X-ray diffraction experiments observed a transition above 45 kbar from the ambient I42M tetragonal space group to monoclinic²⁴⁻²⁶.

Here we present neutron spectroscopy results, which directly determine the pressure dependence of the gap and through the dynamic structure factor allows us to address the nature of the correlations. Figure 1 summarize the phase diagram of $\text{SrCu}_2(\text{BO}_3)_2$, we determined in this study. The exact dimer phase survives up to 16 kbar. The gap decreases from 3 meV to 2 meV, but does not vanish. At 21.5 kbar we discover experimentally a new, intermediate phase. We identify it by its inelastic neutron scattering spectrum as the formation of 4-spin plaquette singlets. Above 40 kbar and below

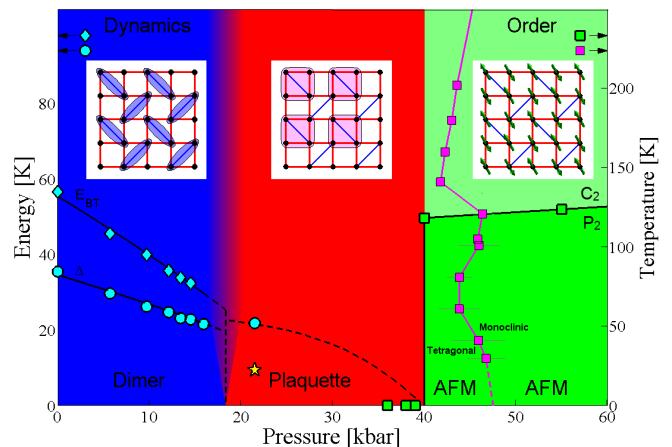


FIG. 1. Phase diagram of $\text{SrCu}_2(\text{BO}_3)_2$ as a function of pressure and temperature, including excitation energies. The blue region is the dimer phase, the red region the newly identified plaquette phase, and the green region the antiferromagnetic phases where $Q=(1,0,0)$ magnetic Bragg peaks, indicated by green squares, are observed only above 40 kbar. Circles are the triplet gap energy Δ at $Q=(2,0,L)$, diamonds are the corresponding 2-triplet bound state energy E_{BT} and the star is a new low energy excitation observed at $Q=(1,0,1)$. The magenta line shows the tetragonal to monoclinic structural transition²⁵. The corresponding monoclinic space groups are indicated^{26,27}. The dashed line in the plaquette phase is the extrapolated energy gap using Ref. 8. The insets depict the corresponding ground states. All the experimental points are from this study.

117 K we find by neutron diffraction that AFM order appears while the compound likely still has tetragonal symmetry with orthogonal dimers. Above ~ 45 kbar, a structural distortion takes place and the symmetry becomes monoclinic, implying non-orthogonal dimers^{25,26}. $\text{SrCu}_2(\text{BO}_3)_2$ is magnetically ordered after the distortion, but can no longer be described appropriately by the original Shastry-Sutherland model. The transition from 2-spin dimer to 4-spin plaquette singlets appears to be of first order, whereas the transition from the plaquette to the AFM phase could be of second order and concomitant with the continuous closure of the plaquette gap or of first order^{8,17,28,29}.

To allow a quantitative comparison to theoretical predictions we establish the pressure dependence of the exchange parameters $J_x(p)$, $J'_x(p)$, and $\alpha(p)$ by measuring magnetic susceptibility $\chi(p, T)$ and fitting it using 20 sites exact-diagonalization. The peak in susceptibility shifts to lower temperature as pressure increases up to 10 kbar (Figure 2a). This suggest a reduction of the spin gap. We parametrise the pressure dependence of J and J' by linear fits (Figure 2b). J has the larger slope so that α increases with pressure. Having established $\alpha(p)$ we see that the critical pressure lying between 16 kbar and 21.5 kbar corresponds to $0.66 < \alpha_c < 0.68$, in good agreement with theoretical predictions^{3,11,17}.

A selection from the neutron spectra leading to the

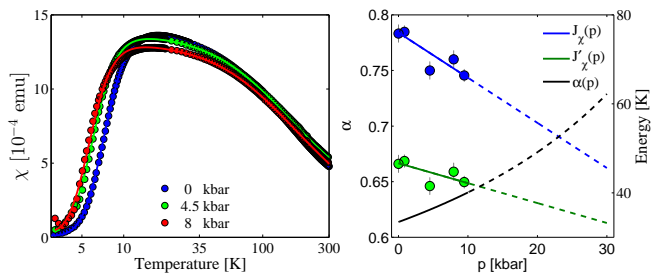


FIG. 2. Pressure dependence of the magnetic susceptibility and of the exchange parameters in $\text{SrCu}_2(\text{BO}_3)_2$. Left, magnetic susceptibility at three pressures below 10 kbar with fits to calculations by exact diagonalization (solid lines), $H=0.5$ T. Right, extracted exchange parameters $J_\chi(p)$ and $J'_\chi(p)$ with linear fits and their ratio $\alpha(p)$.

phase diagram are summarised in Figure 3. Up to 16 kbar an essentially Q -independent linear decrease of the gap energy is observed (Figures 1 and 3a). The measurement of the dispersion and of the structure factor in that pressure range shows that the spin system is still in its original "exact dimer" ground-state with a reduced energy scale of the exchange parameters. The dispersion increases slightly with pressure (not shown), which can be understood by the increase of α^5 . Interestingly, the bound triplet energy E_{BT} softens twice as fast, implying that the triplet binding energy, $\delta = 2\Delta - E_{BT} = 1.19(2)$ meV, remains pressure independent. This results in the unusual situation that extrapolating the softenings, the bound triplet would reach zero energy before the single triplet, and hence that, before that point, exciting a bound state of two triplets would cost less energy than exciting one triplet.

$\text{SrCu}_2(\text{BO}_3)_2$ enters a new quantum phase between 16 and 21.5 kbar, where a discontinuity in the gap softening occurs. The spectra at these two pressures for $Q=(1.5,0,1)$ (Figure 3b) and for $(2,0,0)$ are extremely similar and the gap energy $\Delta \simeq 2$ meV remains unchanged. The transition to a new quantum phase is further asserted by a new type of excitation suddenly appearing at the higher pressure (Figure 3c). It is clearly visible around 1 meV for $Q=(1,0,1)$, $(-1,0,1)$ and $(1,0,1.5)$ at 0.5 K and is not observed at 15 K, which proves the magnetic origin. Figures 3e and 3f show the dispersion and intensity of the two excitations along $(1 \leq H \leq 2, 0, 1)$. The excitation at 2 meV clearly displays a similar behaviour as that expected from the singlet-triplet gap excitation in the exact dimer phase (given by the full lines) and we thus keep labelling it Δ . The new low energy excitation (LE) on the other hand is more dispersive, ~ 0.4 meV in the measured momentum range, and has a different structure factor strongly peaking at $Q=(1,0,1)$. Another strong evidence for the similarity of Δ and the ambient pressure gap is given by the comparison of scans at constant energy along $(H,0,1)$ at 0 and 21.5 kbar in Figure 3d. Except for the overall decrease in intensity, the two scans are close to identical.

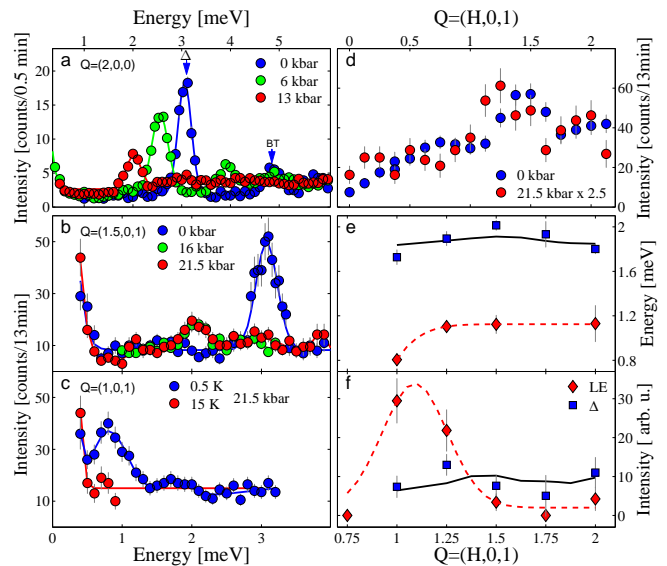


FIG. 3. Inelastic neutron scattering measurements of $\text{SrCu}_2(\text{BO}_3)_2$ under hydrostatic pressure. (a) Energy spectra with triplet gap Δ and 2-triplet bound state E_{BT} energies softening in the dimer phase (setup 1). (b) Discontinuity in the gap softening at 16 and 21.5 kbar (setup 2). (c) New low energy excitation LE at $Q=(1,0,1)$ (setups 2,3). (d) Momentum dependence at the gap energy Δ (setup 2). (e-f) Dispersion and intensity for the triplet Δ and LE, the solid lines are scaled ambient pressure values adapted from³⁰ and the dashed lines are guides to the eye.

To interpret the appearance of a new excitation and the observed momentum dependence of the dynamical structure factors, it is illustrative to consider the simplified case of an isolated 4-spin plaquette, described in the Methods section, which has a singlet ground state and shows two low lying excitations T_1 and T_2 . The structure factors of these excitations, summed over the two possible 'full' plaquette orientations (Figure 4a), are shown in Figures 4b-c together with those of a 'void' plaquette (Figures 4d-f) containing no diagonal bond. T_1 has a structure factor peaking near $Q_{hk}=(Q_h, Q_k)=(1,0)$ in the 2D geometry of $\text{SrCu}_2(\text{BO}_3)_2$ for both full and void plaquettes (Figure 4g). T_2 , however, has a structure factor identical to that of an isolated dimer on the diagonal bond only for the full plaquette (Figures 4c, 4f, and 4h). While an extended many-body calculation would be needed for a fully quantitative comparison, the isolated plaquette considered here displays the main characteristics of the new intermediate pressure phase: (1) a non-magnetic gapped ground state, (2) a low energy triplet (LE) with structure factor peaking at $Q_{hk}=(1,0)$, and (3) another low energy excitation (Δ) with structure factor identical to the singlet-triplet transition in the exact dimer phase. We thus identify the discovered phase as composed of 4-spin plaquette singlets, with excitation LE corresponding to T_1 and

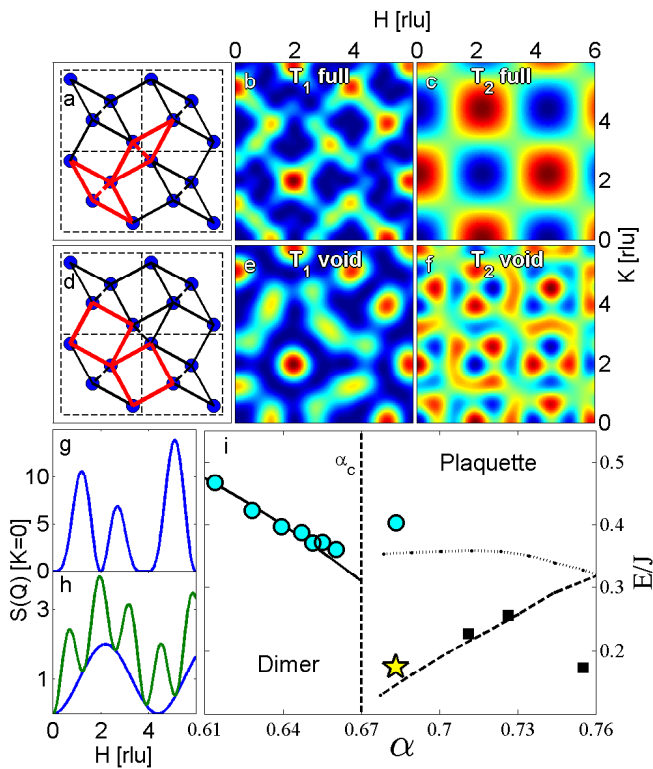


FIG. 4. Plaqueette phase in $\text{SrCu}_2(\text{BO}_3)_2$. (a,d) Plaqueettes containing a diagonal bound (full plaqueettes) and void plaqueettes. The structure factors $S^{xx} + S^{yy} + S^{zz}$ for T_1 (b,e) and T_2 (c,f) are calculated as the sum over the two possible plaqueette orientations in the $\text{SrCu}_2(\text{BO}_3)_2$ geometry and (c) is identical to the structure factor of two orthogonal isolated dimers. (g) Structure factor along $Q_{hk} = (Q_h, Q_k) = (H, 0)$ for T_1 . Void and full plaqueette are identical. (h) Structure factor along $Q_{hk} = (H, 0)$ for T_2 , void plaqueette in green and full plaqueette in blue. The blue line is also the isolated dimer structure factor. (i) Comparison of excitation energies between experiment (same points as in Fig. 1) and theory calculations: dimer gap energy adapted from Ref. 10 (full line), low and high energy triplet excitations in the plaqueette phase from Ref. 9 (dotted lines), and for columnar plaqueette block energies Ref. 12 (black squares).

excitation Δ corresponding to T_2 . Comparing the experimental intensities to this simple calculation favors the singlets sitting on ‘full’ plaqueettes containing diagonal bonds, but calculations of the structure factor for the extended model are required for verification of this point.

To analyze further the interacting plaqueette system, we plot in Figure 4i the measured energies E/J vs. α which enables a direct comparison between our results and the calculations for the low- and high-energy RVB-like plaqueette excitations by Ref. 9, and columnar plaqueette block energy¹². Experimental and calculated⁵ gap energies in the dimer phase are in excellent agreement. Beyond the transition, there is qualitative agreement for the energy scales, in particular the observed energies of LE and of Δ for 21.5 kbar are close to the expected low- and high-energy plaqueette excitations of Ref. 9 for $\alpha = 0.68$.

Our results can also explain the occurrence of magnetic ordering proposed by NMR measurements at 24 kbar and 7 T²²: the new spin $S=1$ excitation LE being low in energy (0.5 meV), a 7 T field is sufficient to close the related gap and to obtain a magnetic ground state. This field-induced quantum critical point and resulting phase will be related to the field-induced BEC physics observed in dimer singlet systems³¹, but could reveal new phenomena due to the strong frustration in the Shastry-Sutherland model. Especially, the evolution of the magnetisation plateaus in $\text{SrCu}_2(\text{BO}_3)_2$ with pressure remains to be studied. Based on our results presented here we can predict that in particular the pressure range between 15 and 25 kbar will be of high interest.

In conclusion we have performed high pressure experiments on $\text{SrCu}_2(\text{BO}_3)_2$ and tuned the compound to experimentally identify a plaqueette singlet phase at intermediate exchange ratio in the Shastry-Sutherland lattice. We observed a first order transition taking place between two magnetically disordered states: the exact 2-spin dimer singlet and the 4-spin plaqueette singlet phase. The dominant correlations in the plaqueette phase involve a four-spin unit and are characterised by a low-lying triplet excitation that is not present in the dimer phase and that gives access to new types of field- and pressure-induced quantum critical points. The plaqueette phase itself is suppressed at higher pressures where classical Néel order is found. Particularly exciting is the fact that the existence of two possible plaqueette singlet coverings offer an Ising-type order parameter. This may turn the transition from plaqueette to Néel phase into a deconfined quantum critical point at 40 kbar.

¹ Lhuillier, C. & Misguich, G. Frustrated quantum magnets. In Berthier, C., Lvy, L. & Martinez, G. (eds.) *High Magnetic Fields*, vol. 595 of *Lecture Notes in Physics*, 161–190 (Springer Berlin Heidelberg, 2001).

² Shastry, B. S. & Sutherland, B. Exact ground state of a quantum mechanical antiferromagnet. *Physica B+C* **108**, 1069 – 1070 (1981).

³ Miyahara, S. & Ueda, K. Theory of the orthogonal dimer Heisenberg spin model for $\text{SrCu}_2(\text{BO}_3)_2$. *J. Phys. Condens. Matter* **15**, R327 (2003).

⁴ Albrecht, M. & Mila, F. First-order transition between magnetic order and valence bond order in a 2D frustrated Heisenberg model. *EPL (Europhysics Letters)* **34**, 145 (1996).

- ⁵ Weihong, Z., Hamer, C. J. & Oitmaa, J. Series expansions for a Heisenberg antiferromagnetic model for $\text{SrCu}_2(\text{BO}_3)_2$. *Phys. Rev. B* **60**, 6608–6616 (1999).
- ⁶ Müller-Hartmann, E., Singh, R. R. P., Knetter, C. & Uhrig, G. S. Exact Demonstration of Magnetization Plateaus and First-Order Dimer-Néel Phase Transitions in a Modified Shastry-Sutherland Model for $\text{SrCu}_2(\text{BO}_3)_2$. *Phys. Rev. Lett.* **84**, 1808–1811 (2000).
- ⁷ Knetter, C., Bühler, A., Müller-Hartmann, E. & Uhrig, G. S. Dispersion and Symmetry of Bound States in the Shastry-Sutherland Model. *Phys. Rev. Lett.* **85**, 3958–3961 (2000).
- ⁸ Koga, A. & Kawakami, N. Quantum Phase Transitions in the Shastry-Sutherland Model for $\text{SrCu}_2(\text{BO}_3)_2$. *Phys. Rev. Lett.* **84**, 4461–4464 (2000).
- ⁹ Takushima, Y., Koga, A. & Kawakami, N. Competing Spin-Gap Phases in a Frustrated Quantum Spin System in Two Dimensions. *J. Phys. Soc. Jpn.* **70**, 1369–1374 (2001).
- ¹⁰ Zheng, W., Oitmaa, J. & Hamer, C. J. Phase diagram of the Shastry-Sutherland antiferromagnet. *Phys. Rev. B* **65**, 014408 (2001).
- ¹¹ Läuchli, A., Wessel, S. & Sigrist, M. Phase diagram of the quadrumerized Shastry-Sutherland model. *Phys. Rev. B* **66**, 014401 (2002).
- ¹² Al Hajj, M. & Malrieu, J.-P. Phase transitions in the Shastry-Sutherland lattice. *Phys. Rev. B* **72**, 094436 (2005).
- ¹³ Majumdar, C. K. & Ghosh, D. K. On Next Nearest Neighbor Interaction in Linear Chain. I. *J. Math. Phys.* **10**, 1388–1398 (1969).
- ¹⁴ Dalla Piazza, B. *et al.* Fractional excitations in the square-lattice quantum antiferromagnet. *Nature Phys.* **11**, 62–68 (2015).
- ¹⁵ Momoi, T. & Totsuka, K. Magnetization plateaus of the Shastry-Sutherland model for $\text{SrCu}_2(\text{BO}_3)_2$: Spin-density wave, supersolid, and bound states. *Phys. Rev. B* **62**, 15067–15078 (2000).
- ¹⁶ Dorier, J., Schmidt, K. P. & Mila, F. Theory of Magnetization Plateaus in the Shastry-Sutherland Model. *Phys. Rev. Lett.* **101**, 250402 (2008).
- ¹⁷ Corboz, P. & Mila, F. Tensor network study of the Shastry-Sutherland model in zero magnetic field. *Phys. Rev. B* **87**, 115144 (2013).
- ¹⁸ Senthil, T., Vishwanath, A., Balents, L., Sachdev, S. & Fisher, M. P. A. Deconfined Quantum Critical Points. *Science* **303**, 1490–1494 (2004).
- ¹⁹ Merchant, P. *et al.* Quantum and classical criticality in a dimerized quantum antiferromagnet. *Nature Phys.* **10**, 373–379 (2014).
- ²⁰ Kageyama, H., Mushnikov, N. V., Yamada, M., Goto, T. & Ueda, Y. Quantum phase transitions in the orthogonal dimer system $\text{SrCu}_2(\text{BO}_3)_2$. *Physica B* **329-333**, 1020 – 1023 (2003).
- ²¹ Sakurai, T. *et al.* High-field and high-pressure ESR measurements of $\text{SrCu}_2(\text{BO}_3)_2$. *J. Phys. Conf. Ser.* **150**, 042171 (2009).
- ²² Waki, T. *et al.* A Novel Ordered Phase in $\text{SrCu}_2(\text{BO}_3)_2$ under High Pressure. *J. Phys. Soc. Jpn.* **76**, 073710 (2007).
- ²³ Haravifard, S. *et al.* Continuous and discontinuous quantum phase transitions in a model two-dimensional magnet. *Proc. Natl. Acad. Sci. USA* **109**, 2286–2289 (2012).
- ²⁴ Loa, I. *et al.* Crystal structure and lattice dynamics of at high pressures. *Physica B* **359-361**, 980 – 982 (2005).
- ²⁵ Zayed, M. *et al.* Temperature dependence of the pressure induced monoclinic distortion in the spin Shastry-Sutherland compound $\text{SrCu}_2(\text{BO}_3)_2$. *Solid State Commun.* **186**, 13 – 17 (2014).
- ²⁶ Haravifard, S. *et al.* Emergence of long-range order in sheets of magnetic dimers. *Proc. Natl. Acad. Sci. USA* **111**, 14372–14377 (2014).
- ²⁷ Zayed, M. *Novel states in magnetic materials under extreme conditions. A high pressure neutron scattering study of the Shastry Sutherland compound $\text{SrCu}_2(\text{BO}_3)_2$* . Ph.D. thesis, ETH Zurich (2010).
- ²⁸ Koga, A., Okunishi, K. & Kawakami, N. First-order quantum phase transition in the orthogonal-dimer spin chain. *Phys. Rev. B* **62**, 5558–5563 (2000).
- ²⁹ Block, M. S., Melko, R. G. & Kaul, R. K. Fate of $\mathbb{C}\mathbb{P}^{N-1}$ Fixed Points with q Monopoles. *Phys. Rev. Lett.* **111**, 137202 (2013).
- ³⁰ Kakurai, K. *et al.* Neutron Scattering Investigation on Quantum Spin System $\text{SrCu}_2(\text{BO}_3)_2$. *Prog. Theor. Phys. Supp.* **159**, 22–32 (2005).
- ³¹ Ruegg, C. *et al.* Bose-Einstein condensation of the triplet states in the magnetic insulator TlCuCl_3 . *Nature* **423**, 62–65 (2003).
- ³² Zayed, M. E. *et al.* Correlated Decay of Triplet Excitations in the Shastry-Sutherland Compound $\text{SrCu}_2(\text{BO}_3)_2$. *Phys. Rev. Lett.* **113**, 067201 (2014).

I. METHODS

Experiments. We measured the excitation spectrum of $\text{SrCu}_2(\text{BO}_3)_2$ by inelastic neutron scattering (INS) on respectively 3 g single crystals up to 15 kbar and 0.2 g at 16 and 21.5 kbar with piston cylinder clamped pressure cells with different experimental setups: Setup 1: IN14 ILL, $k_f=1.3 \text{ \AA}^{-1}$, aluminium-steel pressure cell, $p \leq 17$ kbar (HPCAL17), He-pumped cryostat, $T=1.5$ K. Setup 2: IN14, ILL, $k_f=1.5 \text{ \AA}^{-1}$, McWhan pressure cell, $p \leq 22$ kbar, He-direct flow cryostat, $T=2$ K. Setup 3: Same as setup 2, with ^3He cryostat, $T=0.5$ K. High pressure INS data was also collected with the following setups: Setup 4: TASP, SINQ-PSI, $k_f=1.3 \text{ \AA}^{-1}$, aluminum pressure cell, $p \leq 12$ kbar. Setup 5: PANDA, FRM-2, $k_f=1.5 \text{ \AA}^{-1}$, HPCAL17. Setup 4-5 have He-pumped cryostats, $T=1.5$ K. Given the unusual temperature dependence in $\text{SrCu}_2(\text{BO}_3)_2$, where the INS intensity of the 35 K gap is reduced by half already around 7 K³², we performed the measurements at 21.5 kbar both at 2 K and 0.5 K but no significant change in the excitation intensity was observed. AFM order was observed by neutron diffraction on IN8, ILL, $k_f=2.66 \text{ \AA}^{-1}$, $p \leq 65$ kbar with a Paris-Edinburgh press. Pressure was determined by the shift in lattice constant of Pb or NaCl reference to ~ 0.7 kbar accuracy. The pressure dependence of magnetic susceptibility was measured on a MPMS SQUID magnetometer (Quantum Design) using non-magnetic CuBe clamp pressure cells (CamCell). Pressure was calibrated by the superconducting transition of Pb.

Data analysis. The pressure dependent gap $\Delta(J_\chi(p), J'_\chi(p))$ obtained through the $Q=0$ expansion of Ref. 10 with exchange parameters from fits to susceptibility data is in good agreement with the direct INS gap measurement $\Delta_Q(p)$. To take into account the small Q -dependence of Δ_Q , due to Dzyaloshinskii-Moriya interactions³⁰, we additionally used

$\Delta_Q(p) = \Delta(J_\chi(p), J'_\chi(p)) + D_Q(p)$, where the correction factor D_Q is of the order of 0.2 meV.

The 4-spin plaquette is described by the Hamiltonian:

$$\mathcal{H} = J'(\vec{S}_1\vec{S}_2 + \vec{S}_2\vec{S}_3 + \vec{S}_3\vec{S}_4 + \vec{S}_1\vec{S}_4) + J(\vec{S}_1\vec{S}_3), \quad (1)$$

where the last term represents a diagonal bond between sites 1 and 3 (a 'full' plaquette), and should be removed for a 'void' plaquette without such a diagonal bond. The eigenstates of \mathcal{H} can be separated over two sectors depending on the value of the quantum number $S_{1,3}$ for the spins $\vec{S}_1 + \vec{S}_3$ on the diagonal bond and $S_{2,4}$ for the spins $\vec{S}_2 + \vec{S}_4$ on the outer sites^{27,28}. A study of the excitation spectrum of such a plaquette shows that for $\alpha \geq 0.5$ the ground state is an $S=0$ singlet of four spins. Two low-lying excitations T_1 and T_2 are present. For $\alpha \geq 1$, T_1 has the lower energy, while for $0.5 \geq \alpha \geq 1$ T_2 does. T_1 corresponds to a triplet excitation with both $S_{1,3}$ and $S_{2,4}$ equal to 1. In the full plaquette, T_2 is four-fold degenerate and corresponds to a singlet on the diagonal $S_{1,3}=0$ plus two free spins, $S_{2,4}=0$ or 1. The corresponding structure factor is identical to that of the singlet-triplet excitation on the isolated diagonal bond. For the void plaquette, T_2 is sevenfold degenerate and the structure factor does not match the isolated dimer.

II. ACKNOWLEDGMENTS

We thank A. Magee for her contributions to the susceptibility measurements, M. Merlini and M. Hanfland for support

during high-pressure X-ray diffraction experiments at the ESRF, and M. Ay and P. Link for assistance during neutron scattering experiments. We acknowledge F. Mila and B. Normand for many useful discussions. This work is based on experiments performed at the Swiss spallation neutron source SINQ, Paul Scherrer Institute, Villigen, Switzerland, at the FRM-2, Munich, Germany, and at the ILL, Grenoble, France. We thank the Swiss National Science Foundation SNF and the Royal Society (UK) for financial support. J.L.J. also acknowledges CNPq/MCTI.

III. AUTHOR CONTRIBUTION

M.E.Z, C.R and H.M.R designed the research, performed the experiments and analyzed the data. A.L. computed the magnetic susceptibility by exact diagonalization. C.P, S.S.S and M.E helped with susceptibility experiments. S.S.S, T.S, S.K, G.H and R.A.S provided neutron high pressure techniques. M.B, M.J.R, A.S, V.P. and T.S. provided support for neutron experiments. E.P, M.S., and K.C. synthesized the $\text{SrCu}_2(\text{BO}_3)_2$ samples. J.L.J. and D.M. contributed to interpretation of the data. M.E.Z, C.R and H.M.R wrote the manuscript with contributions from all co-authors.